Flexible membranes anchored to the ground for slope stabilisation: numerical modelling of soil slopes using SPH.

Blanco-Fernandez, E [a, *]; Castro-Fresno, D. [a]; del Coz Diaz, Juan Jose [b]; Navarro-Manso, A [b]; Alonso-Martinez, M. [b]

[a] GITECO Research Group, Universidad de Cantabria. Avenida de los Castros s/n. 39005 Santander, Spain.

[b] Area of Construction Engineering, EPSIG, University of Oviedo, Edificio Oeste N° 7 Dpcho.7.1.02, Campus de Gijón, 33204 Gijón, Spain.

[*] Corresponding author: elena.blanco@unican.es

Abstract

An alternative modelling for flexible membranes anchored to the ground for soil slope stabilisation is presented using Smoothed-Particle Hydrodynamics to model the unstable ground mass in a soil slope, employing a dynamic solve engine. A regression model of pressure normal to the ground, q_{sim}, and also membrane deflection, f_{sim}, have been developed using Design of Experiment. Finally, a comparison between the pressure obtained from numerical simulation and from a limit equilibrium analysis considering infinite slope has been carried out, showing differences in the results, mainly due to the membrane stiffness.

Keywords

Shallow landslides; flexible membranes; cable net; wire mesh, numerical simulation; Smoothed- Particle Hydrodynamics (SPH).

Abbreviations

(Glossary of terms use in formulas, in order of appearance)

q: $Pressure\ normal\ to\ the\ ground\ that\ stabilises\ the\ unstable\ fringe$

c: $Cohesion$

$\emptyset$: $Friction\ angle$

T: $Tensile\ force\ in\ membrane$

$\emptyset_{res}$: $Residual\ friction\ angle$

θ: $Angle\ of\ curvature\ of\ membrane\ with\ respect\ to\ the\ slope\ surface\ in\ the\ bolt\ connection$

l: $Bolt\ spacing$

f: $Maximum\ deflection\ of\ membrane\ in\ the\ normal\ direction\ of\ the\ slope\ surface$

k: $Second\ term\ coefficent\ of\ a\ generic\ parabolic\ curve\ (y = k \cdot x^2)$

e: $Membrane\ thickness\ (considered\ as\ a\ continuos\ shell)$

τ_{max}: $Maximum\ tensile\ stress\ in\ membrane\ (considered\ as\ a\ continuous\ shell)$

ρ: $Soil\ density$

β: $Slope\ angle$

d: $Depth\ of\ unstable\ fringe\ of\ soil$

E_{soil}: $Elastic\ modulus\ of\ soil$

E_{mem}: $Elastic\ modulus\ of\ membrane$

a_i: $Terms\ coefficients\ in\ the\ regression\ models$

p: $Probability\ of\ reject\ a\ term\ in\ the\ regression\ \ model\ although\ it\ is\ significant$

R^2_{adj}: $Determination\ coefficient\ adjusted$

R^2_{pred}: $Determination\ coefficient\ predicted$

H: $Slope\ height$

m: $Mass\ of\ a\ portion\ of\ soil\ in\ the\ unstable\ fringe$

g: $Gravity\ acceleration$

q_{sim}: $Pressure\ normal\ to\ the\ ground\ that\ stabilises\ the\ unstable\ fringe, calculated\ with\ the\ numerical\ simulation$

q_{inf}: $Pressure\ normal\ to\ the\ ground\ that\ stabilises\ the\ unstable\ fringe, calculated\ with\ the\ limit\ equilibrium\ equations$

f_{sim}: $Maximum\ deformation\ of\ the\ membrane, measured\ normal\ to\ the\ ground\ in\ the\ mid\ point\ of\ a\ panel, calculated\ with\ the\ numerical\ simulations$

g_{200}: $Curve\ representing\ the\ regression\ model\ for\ \frac{q_{sim}}{(\gamma \cdot d)}\ when\ E_{mem} = 200\ MPa, based\ on\ numerical\ simulations$

g_{600}: $Curve\ representing\ the\ regression\ model\ for\ \frac{q_{sim}}{(\gamma \cdot d)}\ when\ E_{mem} = 600\ MPa, , based\ on\ numerical\ simulations$

g_{inf}: $Curve\ representing\ \frac{q}{(\gamma \cdot d)} in\ the\ infinite\ slope\ model$

d_{DW}: $Durbin - Watson\ statistic$

$d_{U,\alpha}$: $Durbin - Watson\ upper\ critical\ value$

1.- Introduction

Flexible membranes anchored to the ground constitute a method of the slope surface stabilisation. These membranes are normally made of cable nets, wire meshes or ring nets, bolts anchored to the ground and reinforcement cables forming regular patterns. This technique has been widely used due to its low visual impact and scarce traffic interference during installation.

Flexible membranes may be classified as either low-resistance or high-resistance. A low-resistance membrane is generally formed by a twisted (single, double or triple) hexagonal wire mesh manufactured with standard steel and anchored to the ground at a few points with bolts, allowing material to slide due to a loose contact between the membrane and the slope surface. The main purpose of this type of membrane is to work as a curtain, preventing small rock pieces from getting to the road when they detach by conducting them along the slope surface till the ditch. High-resistance flexible membranes are formed by stiffer membranes (either cable nets, single torsion wire meshes or ring nets), with a relatively more rigid contact to the slope surface. They are manufactured with medium to high strength steel. According to some manufacturers and researchers, the main application of these membranes is to avoid soil sliding or rock detachment in slopes by exerting a pressure, q, normal to the ground surface, which prevents instability by increasing internal shear strength in the sliding plane. This pressure q is generated from a pre-stress force applied to the membrane and reinforcement cables at the time of installation. Manufacturers and researchers usually refer to this behaviour as *'active'*, in a similar way to the concept of *'active anchors'* in the field of soil nailing; in both cases structural elements are pre-stressed.

Although the use of flexible membranes has become very common worldwide, there are only two technical guidance documents that suggest a design methodology (Muhunthan et al. 2005; Phear et al. 2005). There is only one standard document (UNI 11437:2012) that deals with test methods for flexible systems for slope stabilisation; however, design procedures are not described in this document. Moreover, there are only a few scientific references related to the topic of design methodology other than those published by the manufacturers of cable nets and high-resistance wire meshes themselves, and two PhD theses by independent researchers from the University of Cantabria (Castro Fresno 2000; Da Costa García 2004). In most of these previous works, active behaviour was assumed in order to design the flexible system.

A design method of these systems based on passive behaviour was first introduced in Bertolo & Giacchetti (2008). The work described a design procedure for flexible systems anchored to rock slopes in order to retain a rock wedge. The method assumed that a certain deformation of the membrane is necessary in order to develop tensile forces in it, and, therefore, apply a certain pressure on the rock wedge. A limit equilibrium analysis (LE) was performed in two dimensions. Mohr-Coulomb failure criterion was adopted between rock wedge and unstable mass with a friction angle of 45º. The force-displacement curve of the membrane was obtained from a puncture test carried out in laboratory on a square cable net panel of 3m side. This model did not account for the dynamic force of the impact of a moving mass (rock wedge) impacting on the membrane. In addition, residual strength between rock wedge and unstable mass was not considered, which is generally lower than the peak shear strength. In Bertolo et al. (2009), a full scale test method for flexible systems anchored in rock slopes was

presented. In this paper, it was also considered that the membrane had a passive behaviour.

Most manufacturers and independent researchers adopt an active behaviour for these membranes for design purposes; however, this hypothesis was not specifically verified. Most models found in the literature are analytical, except three models proposed by Da Costa García (2004), Luis Fonseca (2010), Sasiharan et al. (2006) using numerical simulations.

Da Costa Garcia (2004) performed a numerical simulation using FEM (Finite Element Method), representing a two-dimension section of the slope. The membrane was represented with an elastic shell component, bolts were represented through points in the membrane where only vertical displacement was allowed. Ground slope was discretised with a Matsuoka-Nakai model with a cohesive soil, where a strength reduction law of cohesion (c) and friction angle (∅) was applied in order to provoke failure. The highest deformations in membrane in the worst situation reached about 4 mm. In the real situation, typical deformations in the membrane could be of 300-500 mm.

Luis Fonseca (2010) published a technical book where practical information about different flexible systems used to prevent rock fall hazards was compiled. In this work, a numerical simulation performed by researchers at the Science and Technology University of Krakow (M. Cala, M. Kowalski) was presented. The researchers perform a comparison using the software FLAC to compare the safety factor of a slope, using only anchors or anchored flexible membranes, to a slope with no protection. The results

provided showed that the safety factor when using anchored membranes was higher than using only anchors, and both clearly higher than not using any protection. However, researchers did not provide any information regarding the tensile stress or deformations in membrane in order to compare the similarity to a real case.

Sasiharan et al. (2006) proposed numerical simulations on a drapery system anchored to the ground. These simulations reproduced only one type of flexible systems which performed as a curtain to prevent debris from reaching the road. Only horizontal reinforcement cables were placed at the top of the slope, in order to allow debris to reach the bottom of the slope. The numerical simulation consists of a membrane panel from the top of the slope to bottom of a certain width in order to be representative. The forces applied were only at the bottom of the membrane, parallel to it and oriented in the downslope direction. Various scenarios were simulated studying the influence of slope angle, bolt spacing and bolts and reinforcement cable arrangement.

Apart from these three examples, most of existing design methods are based on limit equilibrium methods. The main difference between models is whether they consider or not cohesion, pore pressures or seismic forces. Also, there are also some variations in the geometry of the potential failure mass of soil among models: some of them considered wedges, other blocks+wedges and others infinite slopes. In the general case, a uniform pressure q normal to the ground is calculated so that it increases the normal effective stress on the sliding surface and therefore the shear strength on it. Two main conditions have to be satisfied by a flexible membrane to be considered as active (Blanco-Fernandez et al. 2011):

– Condition 1: The membrane (and therefore slope surface) should present a convex shape: either a catenary, circle or parabola.
– Condition 2: The membrane has to be initially pre-stressed with a known tensile force T, which depends on stabilisation pressure *q* and slope curvature.

For the first condition, several field inspections and photo records of real sites show that slopes rarely have a convex shape. The most common shape is flat or in the most favourable case, irregular (flat, convex and concave shape present in the same slope surface). Even if an installer reshaped the slope surface and achieved the desired convex shape, it would be almost impossible to maintain this shape over time due to long-term weathering.

In relation to condition 2, it has been demonstrated that pre-stress in the system components, membrane, reinforcement cables and bolts is very low, so an active behaviour cannot be considered under these conditions (Blanco-Fernandez et al. 2013).

2.- Numerical simulation procedure

2.1.- Methodology. General aspects

It has already been proved that membranes behave passively (Blanco-Fernandez et al. 2011, 2013), which means that they are able to retain an unstable mass (slip circle or rock edge) that has already started to slide. Therefore, the aim of the simulation should be to describe the interaction of a moving mass with the stable portion of the ground and the flexible membrane.

Starting from this alternative approach, the work flow should begin with the definition of the dimensions of the unstable mass of either soil or rock. In both cases, conventional methods that incorporate the possibility of including passive reinforcement could be used. Until the failure criterion is reached, neither membrane nor reinforcement cables would add any notable stabilisation force to the equilibrium of the potential unstable mass. However, anchor bolts might add some strength, due to friction developed along their length and also due to the bending moment and shear strength at their intersection with the potential sliding surface.

Concerning soil slopes, different methods, based on LE methods, have been reported in the literature to obtain the slip surface circle; these include passive reinforcement (Schlosser 1983; Juran et al. 1990; Jewell and Pedley 1990). Also, various solutions have been developed using FEM with a soil strength reduction method and passive reinforcement options (Wei et al. 2008; Wang and Men 2010).

After the size of the unstable mass is obtained by any of the methods discussed above, the dynamic simulation can be set up. A two-dimensional (2D) plane-stress model of a vertical section representing the strip of a ground mass can be established to simulate the slope (see Fig. 1). 2D simulations have an advantage in relation to three-dimensional ones (3D), the saving in computing time; however, certain assumptions have to be adopted (see 2.3.2), which alters the real situation. In contrast, 3D simulation can better describe the real setting of anchors, reinforcement cables, either horizontal or vertical and orthotropic membranes. Nevertheless, assumptions adopted for the 2D

simplification should assume a system that is less restrained in movements than in reality in order to be on the safe side.

Fig. 1. Section of membrane panel represented in simulation

Dynamic simulation with explicit software (Autodyn) has been employed in this work. The only external force is gravity, and the initial velocity of the unstable mass is null. The velocity that could develop in the unstable mass is not very high (< 5 m/s); however, using an implicit method could lead to convergence problems and to an excessive computing time. Explicit analysis can also deal with the high non-linearity of the problem, in terms of geometry and material modelling. Fig. 2 (left) and (right) shows simulation examples for a soil slope and a rock slope respectively.

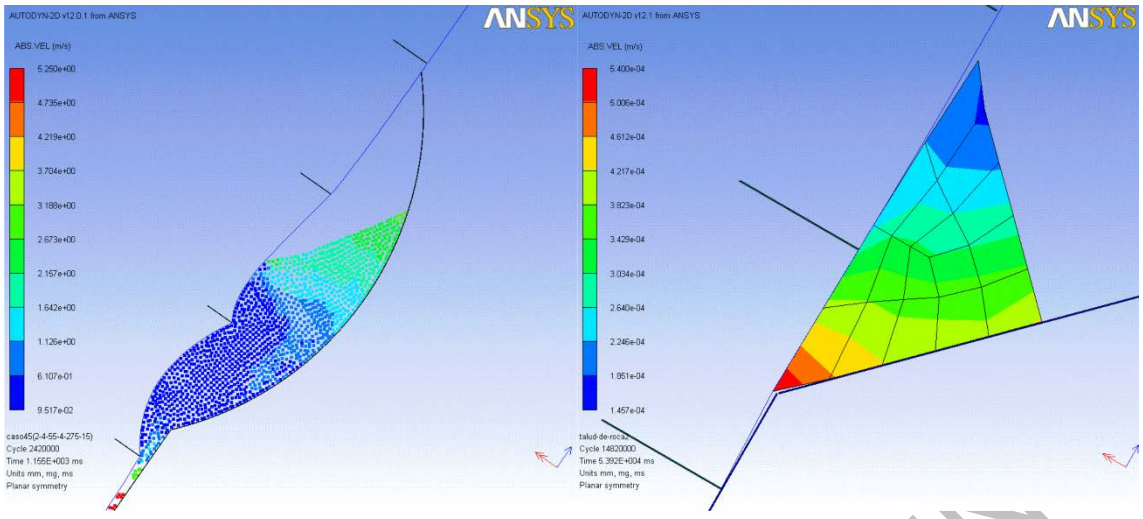

Fig. 2. Numerical simulation example of a flexible membrane. Soil slope (left) and rock slope (right).

During the whole sliding phenomena, a peak force followed by a force stabilisation or decay will appear in the tensile stress in membrane and reinforcement cable due to the impact (Fig. 3).

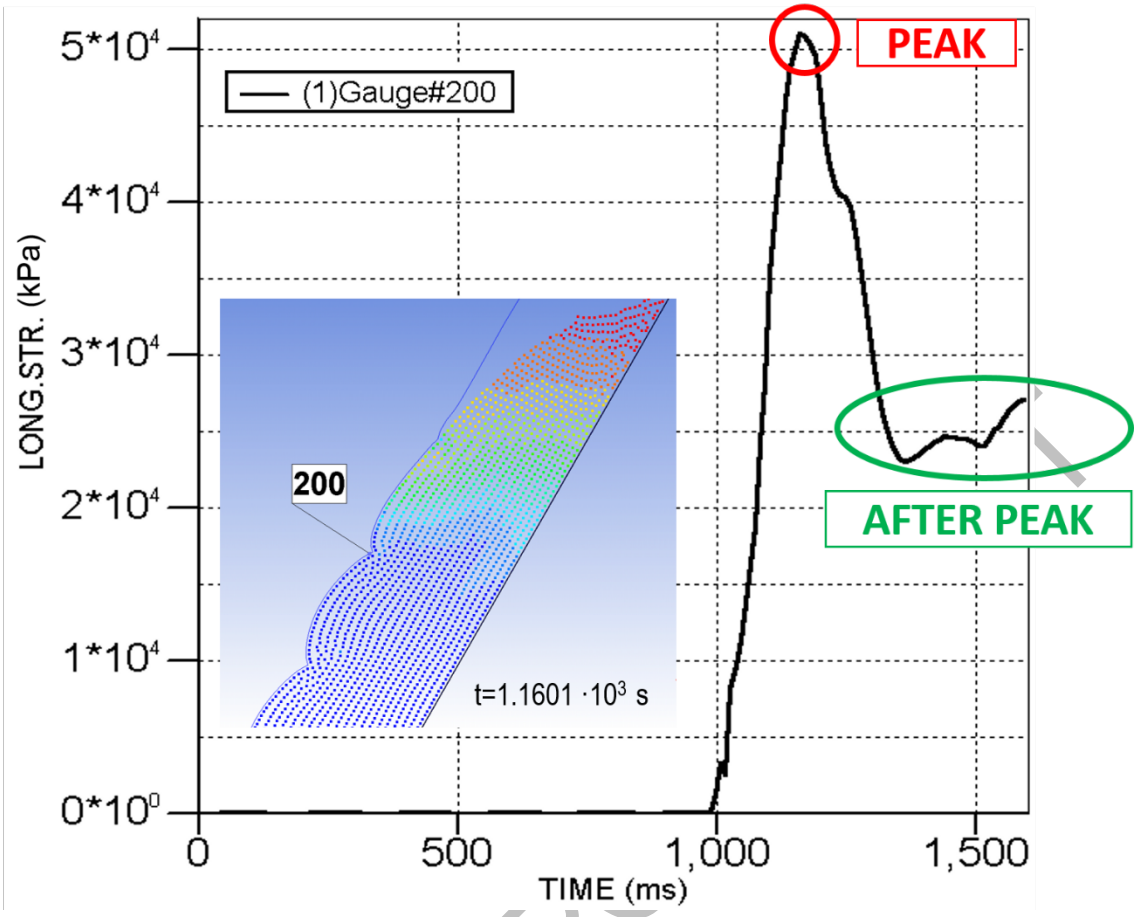

Fig. 3. Tensile stress vs. time (planar failure).

2.2.- Unstable mass formulation for soils

In the particular case of simulation of an unstable soil mass, a type of numerical formulation is desired that allows high deformations and distortions. Various numerical formulations enable high distortions to be dealt with, such as Arbitrary Lagrangian-Eulerian (ALE), Discrete Element Method (DEM) or mesh-less methods such as Smooth Particle Hydrodynamics (SPH), among others. Bojanowski (2014) compared various numerical methods to simulate soil-structure interaction using Finite Element Method (FEM), Element Free-Galerkin (EFM), Smooth Particle Hydrodynamics (SPH) and Multi-Material Arbitrary Lagrangian-Eulerian (MM-ALE). He finally concluded that SPH was more suitable than ALE in terms of its higher ability to model contact

with other Lagrangian components. In relation to computing time, for medium-coarse meshes, SPH was faster than ALE. On the other hand, the main disadvantage of EFM is that it is very rare to find it included in commercial software. Finally, FEM was not recommended for modelling high deformation and high distortion problems.

Bibliographic references concerning comparisons between DEM and SPH to model granular materials have not been found so far. Although soil is a discontinuous medium, classical soil mechanics deals with it as a continuous medium, such as FEM. SPH (Smooth Particle Hydrodynamics) is a Lagrangian mesh free method where a continuous medium is discretised into points (also known as 'particles'), instead of continuous cells or elements. Deformations are expressed in terms of variations of density. For each particle i, density is defined as a simple weighting function of the density of that point i and neighbouring points j and the distance ij. It is generally used to solve free surface problems, fluid problems with a Lagrangian approach, collision or impact problems and large distortion/deformation problems. On the other hand, typical DEM formulations describe interaction between particles as a collision force that includes a linear spring and damping; thus, complex material models are more difficult to model with conventional DEM software.

Bui et al. (2008a) studied for the first time the failure and post-failure mechanism of a soil slope employing SPH discretisation with a Drucker-Prager constitutive model. They presented different simulations considering associated and non-associated plastic flow rules, and different friction angles and cohesion values. They compared the results with scale laboratory test, and also FEM simulations concluding that SPH was an adequate numerical method to simulate both failure and post-failure processes.

On that time, Bui et al. (2008b) performed a numerical simulation of a soil slope discretised with SPH where they introduced a pile in order to study the soil-structure interaction. The slope was first analysed without pile and only gravity as an external force and the results showed a safety factor lower than 1; therefore, failure would occur. Afterwards, the pile was introduced in the slope, and the safety factor increased. No comparisons were performed with laboratory or real cases. However, results apparently show physically logical behaviour.

Later, Bui et al. (2011) resolved a slope stability problem considering also pore water pressures. They compared the results of safety factor and slip surface shape of SPH, FEM and LE showing good agreement. Nevertheless, the authors stress the capability of SPH to simulate the post failure, contrary to the other two methods.

Liang et He (2014) made a simulation using SPH for dry frictional soils in order to analyse the influence of shear rate for different slope angles and depth of the instabilities.

There are also more works after Bui et al. 2008 were the slope failure was modelised using SPH, comparing the results with other methods, laboratory tests or real cases: Nonoyama et al. (2015), Wu et al. (2015), Zhang et al. (2014) and Dakssa & Harahap (2012).

Theoretical limitations of the SPH method are mainly the tension instability that may led to unrealistic soil fracture for large deformations. For only frictional problems with

low friction angles, Bui et al. (2008a) states that the problem of instability is nearly neglectable; besides, for large frictional angles they suggest to use the tension cracking algorithm to overcome the problem of tension instability. In case of cohesive soils, they suggest to use an artificial stress method based on Monaghan (2000) and Grey et al (2001).

To date, there are no studies concerning the simulation of a soil slope discretised with SPH interacting with a flexible membrane.

2.3.- Components of the simulation

2.3.1.- Membrane

The various types of membranes available on the market can be idealised as continuous membranes that only support tensile stress, having different stress-strain characteristics curves and yield criterias. For simulation purposes, it was assumed in this paper that real membranes such as cable nets, wire meshes or ring nets, behave as continuous elastic membranes with a constant elastic modulus.

2.3.2.- Reinforcement cables and bolts

Typical anchoring patterns of both cable nets and wire meshes are formed by square or rectangular panels, limited by rows and columns of bolts (see Fig. 1). Vertical and horizontal reinforcement cables connect anchors and restrain overall membrane deformations.

In this paper, a 2D vertical section passing through the mid-point of two columns of bolts was considered as a representative section for the numerical simulation. In a real situation, the mid-point between two columns of rows shows a certain displacement regarding the stiffness of a horizontal reinforcement cable fixed at two lateral bolts. In order to simplify the model, a null displacement of horizontal cables was considered, represented by a fix point in the numerical simulation.

The 2D simplification of the model (plane stress), implies that only horizontal rows of reinforcement cables/bolts are represented. In the real situation both horizontal and vertical reinforcement cables are generally set up; therefore, the numerical model represents a less restrained situation.

2.3.3.- Stable ground

Stresses in the stable zone of the slope was not relevant for design purposes; so, the only function of the stable slope was to define an interaction surface with the unstable mass. Therefore, the stable slope was represented as a contour surface (only surface stresses have been taken into account) that interacted with the unstable mass with particular friction properties. Some software does not provide the option of boundary surfaces; hence, a Lagrangian discretisation of a thin component representing the stable slope contour would be a suitable alternative.

2.3.4.- Unstable mass: soil slopes

In this article, SPH was proposed as a suitable method considering its adaptability to model high deformation and high distortion problems, its ability to model interactions

with other numerical methods, the possibility to model any type of material behaviours, the affordable computing time and its availability in commercial software. In addition, the works performed in Bui et al. (2008a) and after suggest the suitability of SPH as an alternative tool in the slope stability field.

In relation to the shear strength in the sliding surface it is recommended to use drained residual strength since failure has already been achieved, large shear strains have also appeared, but pore water pressures from stable ground cannot be transmitted anymore to the slip plane. This can be taken into account in Autodyn by introducing a friction coefficient between the unstable mass and ground that should be $tan\,(\emptyset_{res})$. It is important to remark, as well, that Autodyn does not include the possibility of considering cohesion.

2.3.5.- Pore pressures

Current software specialised in geotechnical problems can deal with pore pressures and, therefore, take into account both total and effective stresses. As mentioned in section 2.3.4, one of the possible numerical approaches to deal with large deformations and distortions is SPH. Unfortunately, commercial software including the SPH capability (e.g. Autodyn), is not focused on geotechnical problems; therefore, pore water pressures cannot be taken into account.

3.- Regression model for the numerical simulation results

3.1.- Model for the pressure normal to the ground, q_{sim}

In this section a regression model for the normal pressure applied to ground using the results of numerical simulations based on DOE is presented. The idea is to find out a formula that shows some physical relation between numerical results and some logical input variables.

Regarding limitations in Autodyn, cohesion and pore water pressures have not been taken into account in the numerical simulation, but only friction angle. For the numerical simulation, the pressure q was calculated considering maximum tensile stress and maximum deformation normal to the ground of membrane. Different input variables were considered in order to determine their influence on the pressure q. The pressure q (Eq. 1) was calculated considering that membrane deforms as a parabole (Fig. 4) comprised between two rows of bolts. A 2D balance of equations considering 1 m of slope width was carried out. Membrane thickness was represented through the parameter e.

$$\sum F_y = 0 \;\rightarrow\; 2 \cdot T \cdot sin\theta - q \cdot \mathrm{l} = 0 \rightarrow q = \frac{2 \cdot T \cdot sin\theta}{l}$$

$$y = k \cdot x^2;\; x = \frac{l}{2} \rightarrow f = \frac{k \cdot l^2}{4} \rightarrow k = \frac{4 \cdot \mathrm{f}}{l^2}$$

$$y' = 2 \cdot k \cdot x;\quad x = \frac{l}{2} \rightarrow\; tan\theta = k \cdot l \;\rightarrow\; tan\theta = \frac{4 \cdot \mathrm{f}}{l}$$

$$q = \frac{2 \cdot \tau_{max} \cdot e \cdot sin\left(\mathrm{atan}\left(\frac{4 \cdot f}{l}\right)\right)}{\mathrm{l}} \qquad \text{(Eq. 1)}$$

As shown in Fig. 4, q is the pressure normal to the slope surface per unit of slope width, f is the mid point deflection of the parabole and l is the span of the parabole.

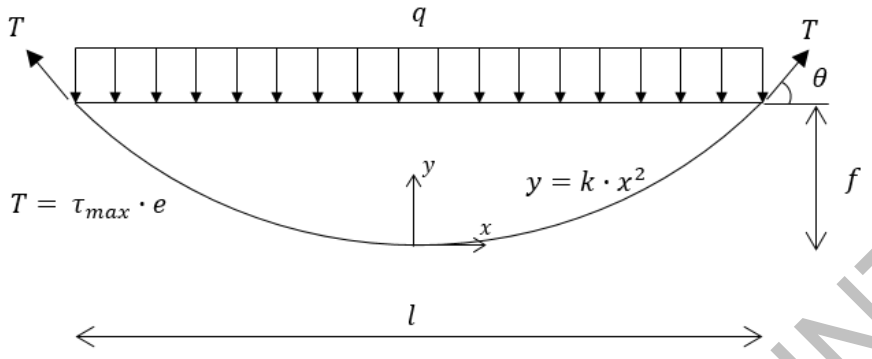

Fig. 4. Tension versus earth pressure in the membrane.

Design of Experiment (DOE) technique was used in order to obtain different ground pressures applied to the membrane in relation to variations of the input variables. The input variables and maximum and minimum values selected for the DOE were shown in Table 1.

Table 1.- DOE: input variables.

Symbol	Variable	Minimum	Maximum
$\emptyset$	Friction angle (º)	10	30
ρ	Soil density (T/m^3)	1.6	2.2
d	Depth of unstable fringe of soil (m)	1	2
β	Slope angle (º)	30	60
E_{soil}	Elastic modulus of soil (kPa)	$5{\cdot}10^3$	$5{\cdot}10^6$
E_{mem}	Elastic modulus of membrane (kPa)	200	600
l	Bolt spacing (m)	2	4

Once the array of scenarios was selected (Table 2), numerical simulations were run in the computer. Two main results were obtained from the numerical simulation: the maximum deformation of membrane (y_{max}) and also the maximum tensile stress on it (τ_{max}). These two values were necessary to calculate the ground pressure q shown in the last column of Table 2, using (Eq. 1. Poisson's ratios have been set to 0.3 for the membrane and 0.22 for the soil. Friction angle between membrane and unstable soil was

set to 25º (Sasiharan et al. 2006). A slope of 30 m length was considered for all simulations.

Fig. 5 shows the process of soil sliding and membrane deformation for run 9. In this case, maximum tensile stress on geomembrane was achieved at 1.4 s. In the image it can be seen that a kind of 'bag' of soil is accumulated between the membrane and the stable slope.

Table 2.- DOE runs and results.

RUN	Ø (º)	ρ (T/m^3)	d (m)	β (º)	E_{soil} (kPa)	E_{mem} (kPa)	l (m)	τ_{max} (kPa)	f_{sim} (m)	q_{sim} (kPa)
1	10	1.6	1	30	$5{\cdot}10^3$	200	2	$9.778{\cdot}10^3$	0.227	40.48
2	30	1.6	1	30	$5{\cdot}10^6$	200	4	$1.855{\cdot}10^2$	0.036	0.03
3	10	2.2	1	30	$5{\cdot}10^6$	600	2	$7.819{\cdot}10^3$	0.191	27.84
4	30	2.2	1	30	$5{\cdot}10^3$	600	4	$5.360{\cdot}10^2$	0.027	0.07
5	10	1.6	2	30	$5{\cdot}10^6$	600	4	$2.498{\cdot}10^4$	0.388	45.12
6	30	1.6	2	30	$5{\cdot}10^3$	600	2	$1.395{\cdot}10^2$	0.002	0.00
7	10	2.2	2	30	$5{\cdot}10^3$	200	4	$2.447{\cdot}10^4$	0.678	68.63
8	30	2.2	2	30	$5{\cdot}10^6$	200	2	$1.003{\cdot}10^2$	0.002	0.00
9	10	1.6	1	60	$5{\cdot}10^3$	600	4	$4.458{\cdot}10^4$	0.603	115.04
10	30	1.6	1	60	$5{\cdot}10^6$	600	2	$4.992{\cdot}10^3$	0.068	6.74
11	10	2.2	1	60	$5{\cdot}10^6$	200	4	$1.848{\cdot}10^4$	0.520	42.64
12	30	2.2	1	60	$5{\cdot}10^3$	200	2	$1.251{\cdot}10^4$	0.247	55.46
13	10	1.6	2	60	$5{\cdot}10^6$	200	2	$1.708{\cdot}10^4$	0.262	79.28
14	30	1.6	2	60	$5{\cdot}10^3$	200	4	$2.048{\cdot}10^4$	0.641	55.25
15	10	2.2	2	60	$5{\cdot}10^3$	600	2	$5.089{\cdot}10^4$	0.300	262.09
16	30	2.2	2	60	$5{\cdot}10^6$	600	4	$1.425{\cdot}10^4$	0.287	19.66
17	20	1.9	1.5	45	2502500	400	3	$1.572{\cdot}10^4$	0.287	37.39

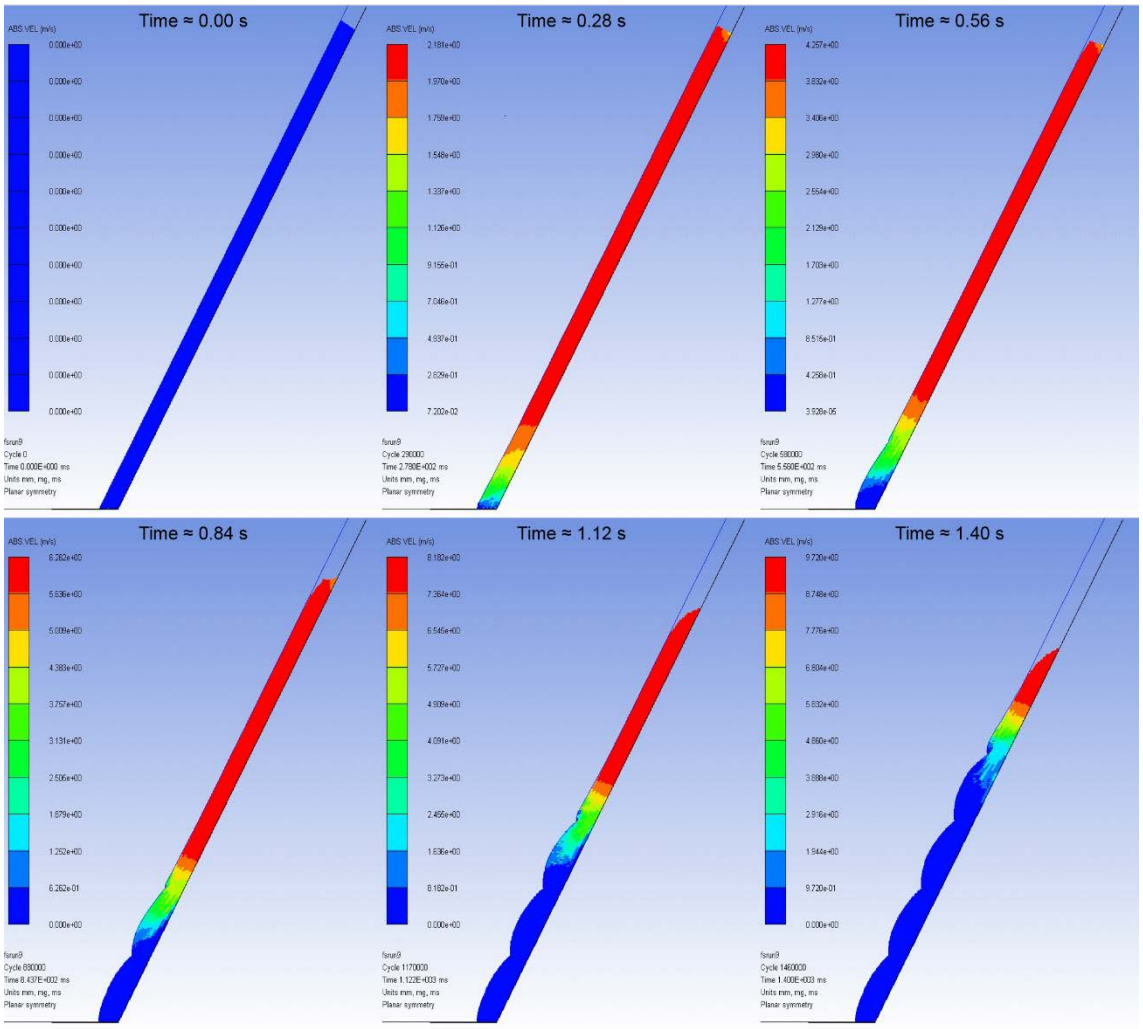

Fig. 5. Numerical simulation evolution of run 9

Table 3.- Regression models for q_{sim} (in bold, selected model)

Model	Description	R^2_{adj}	R^2_{pred}
1	$q_{sim} = a_0 + a_1 \cdot \emptyset + a_2 \rho + a_3 \cdot d + a_4 \cdot \beta + a_5 \cdot E_{soil} + a_6 \cdot E_{mem} + a_7 \cdot l$ $p_{a0} = 0.721$ $p_\emptyset = 0.012$ $p_\rho = 0.459$ $p_\rho = 0.198$ $p_\beta = 0.028$ $p_{E_{soil}} = 0.059$ $p_{E_{mem}} = 0.458$ $p_l = 0.489$	52.89	-3.72
2	$q_{sim} = a_0 + a_1 \cdot \emptyset + a_2 \cdot \rho + a_3 \cdot d + a_4 \cdot \beta$ $p_{a0} = 0.508$ $p_\emptyset = 0.015$ $p_\rho = 0.499$ $p_d = 0.234$ $p_\beta = 0.037$	41.90	9.04
3	$q_{sim} = a_0 + a_1 \cdot \emptyset + a_2 \cdot \rho + a_3 \cdot d + a_4 \cdot \beta + a_5 \cdot E_{mem}$ $p_{a0} = 0.433$ $p_\emptyset = 0.019$ $p_\rho = 0.510$ $p_d = 0.246$ $p_\beta = 0.042$ $p_{E_{mem}} = 0.509$	32.90	-5.40
4	$q_{sim} = a_0 + a_1 \cdot \emptyset + a_2 \cdot \beta$ $p_{a0} = 0.474$ $p_\emptyset = 0.014$ $p_\beta = 0.034$	41.67	23.48
5	$q_{sim} = a_0 + a_1 \cdot x_1 + a_2 \cdot x_2$ $x_1 = \frac{sin\beta}{tan\emptyset}$ $x_2 = cos\beta$ $p_{a0} = 0.662$ $p_{x1} = 0.008$ $p_{x2} = 0.412$	45.46	22.37
6	$q_{sim} = a_0 + a_1 \cdot x_1 + a_2 \cdot x_2$ $x_1 = \frac{d \cdot \rho \cdot sin\beta}{tan\emptyset}$ $x_2 = d \cdot \rho \cdot cos\beta$ $p_{a0} = 0.806$ $p_{x1} = 0.000$ $p_{x2} = 0.165$	70.62	42.62
7	$q_{sim} = a_0 + a_1 \cdot x_1 + a_2 \cdot x_2$ $x_1 = \frac{d \cdot \gamma \cdot sin\beta \cdot E_{mem}}{tan\emptyset}$ $x_2 = d \cdot \gamma \cdot cos\beta \cdot E_{mem}$ $p_{a0} = 0.009$ $p_{x1} = 0.000$ $p_{x2} = 0.000$	89.62	81.82
8	$\boldsymbol{q_{sim} = a_1 \cdot x_1 + a_2 \cdot x_2}$ $\boldsymbol{x_1 = \frac{d \cdot \gamma \cdot sin\beta \cdot E_{mem}}{tan\emptyset}}$ $\boldsymbol{x_2 = d \cdot \gamma \cdot cos\beta \cdot E_{mem}}$ $\boldsymbol{p_{x1} = 0.000}$ $\boldsymbol{p_{x2} = 0.000}$	**89.79**	**89.63**
9	$q_{sim} = a_0 + a_1 \cdot x_1 + a_2 \cdot x_2$ $x_1 = \frac{d \cdot \rho \cdot sin\beta \cdot E_{mem} \cdot E_{soil}}{tan\emptyset}$ $x_2 = d \cdot \rho \cdot cos\beta \cdot E_{mem} \cdot E_{soil}$ $p_{a0} = 0.008$ $p_{x1} = 0.470$ $p_{x2} = 0.272$	-1.79	-12.92

10	$q_{sim} = a_0 + a_1 \cdot x_1 + a_2 \cdot x_2$ $x_1 = \frac{d \cdot \rho \cdot sin\beta \cdot E_{mem}}{tan\emptyset \cdot l}$ $x_2 = \frac{d \cdot \rho \cdot cos\beta \cdot E_{mem}}{l}$ $p_{a0} = 0.003$ $p_{x1} = 0.000$ $p_{x2} = 0.001$	87.06	78.38

Table 3 shows the different regression models of the maximum pressure normal to the ground, q, that were generated in order to see their goodness of fitness for the 17 runs carried out. Maximum pressure (q_{sim}) was adopted as the response of the model. For every model the polynomial expression and also the $'p'$ value of each component (probability to reject that factor from the model though it is significant) are represented. A $'p'$ value equal or lower to 0.05 means that the term is representative in the model, with only a probability of 5% or less not to have any influence in the response. Also, for each model the determination coefficient adjusted (R^2_{adj}) and the determination coefficient predictive (R^2_{pred}) are also shown. Model 8 shows the highest values of R^2_{adj} (89.79%) and R^2_{pred} (89.63%) from all models. In addition, all its input variables are representative in the model. It is important to remark that the expression is similar to the one for the infinite slope (Eq. 4) in a LE analysis, but with different coefficients and also adding as a multiplier factor in both terms E_{mem}.

The final expression, considering the coefficients obtained from the regression model is:

$$q_{sim} = 0.023497 \cdot d \cdot \rho \cdot sin(\beta)/tan(\emptyset) \cdot E_{mem} - 0.0321241 \cdot d \cdot \rho \cdot cos(\beta) \cdot E_{mem}$$

$$\boldsymbol{q_{sim} = d \cdot \rho \cdot E_{mem} \cdot [0.02350 \cdot sin(\beta)/tan(\emptyset) - 0.03212 \cdot cos(\beta)]} \quad \text{(Eq. 2)}$$

The units use for the regression model are metres for d, T/m^3 for ρ and kPa for E_{mem}. The results for q_{sim} will be expressed in kPa according to the coefficients used.

Table 4 shows the fulfilment of the 6 conditions for linear regression models. All hypothesis tests and regression models have been stabilised with 5% of significance level. It is also relevant to outstand that the last test (Independence of predictive variables among them) shows a value higher but very close to 0.05. This result might suggest that predictive variables might be correlated. This could be justified regarding the specific values selected for the DOE; nevertheless, x_1 and x_2 cannot be correlated since in one term there exists $tan(\emptyset)$ while in the other it does not.

Table 4.- Regression model $of\ q_{sim}\ vs. x_1, x_2$: conditions fulfilment

Hypothesis	**Type of test**	**Criteria**	**Value**	**Fulfil?**
Normality of error distribution	Normality test (Anderson-Darling)	p > 0.05	p = 0.850	Yes
Null average of errors	Statistical hypothesis test H_0: μ_{errors} =0	p > 0.05	p = 0.174	Yes
Independence of errors in relation to response	Regression model between errors and response	p > 0.05	p = 0.226	Yes
Independence of errors in relation to predictive variables (homoscedasticity)	Regression model between errors and predictive variables	p > 0.05	p = 1.000	Yes
Independence of errors among them	Durbin-Watson ($d_{U\alpha}$=1.54)	d > $d_{U\alpha}$ 4-d > $d_{U\alpha}$	d = 1.758	Yes
Independence of predictive variables among them	Regression model between predictive variables	p > 0.05	p = 0.057	Yes

The model obtained reveals that variables like l (separation between rows of bolts) and E_{soil} (elastic modulus of soil) do not have a significant influence in the response.

A possible explanation for the lack of influence of E_{soil} in q_{sim}, could be the fact that the deformation of the unstable mass as a whole is more influenced by internal failures that provokes separation of particles and thus large displacements and distortions of the whole unstable mass, rather than E_{soil} itself.

Regarding the apparent lack of influence of l in relation to q_{sim}, it is an unexpected outcome, since from a physical point of view, there should exist some influence. A possible explanation to this finding could be the small number of runs; this may sometimes cause that certain correlations could not be detected. Therefore, in order to have a more clearer conclusion about the influence or not of l, further simulations should be carried out.

3.2.- Model for the membrane deformation, f_{sim}

In this section a regression model for the maximum deformation on membrane, f_{sim}, is proposed. The values considered to perform the regression models were those referred as f_{sim} in Table 2. Eleven different regression models (Table 5) have been generated based on potential input variables. A total of nine input variables have been selected for the first model, which includes the same seven variables $(\emptyset, \rho, d, \beta, E_{soil}, E_{mem})$ that were selected for the q_{sim} model, but adding two more: q_{sim} itself and also τ_{max}. Although these two last variables are obviously correlated among them and also with the previous seven variables, it was decided to include them in the model in order to find out the simplest and more representative regression model. The analysis of the p-value of the terms of each regression model will finally determine which input variables are the most influential. The model with the highest R^2_{adj} and R^2_{pred} is Model 10.

Table 5.- Regression models for f_{sim} (in bold, selected model)

Model	Description	R^2_{adj}	R^2_{pred}
1	$f_{sim} = a_0 + a_1 \cdot \emptyset + a_2 \cdot \rho + a_3 \cdot d + a_4 \cdot \beta + a_5 \cdot E_{soil} + a_6 \cdot E_{mem} + a_7 \cdot l + a_8 \cdot q_{sim} + a_9 \cdot \tau_{max}$ $p_{a0} = 0.867$ $p_\emptyset = 0.099$ $p_\rho = 0.383$ $p_d = 0.208$ $p_\beta = 0.125$ $p_{E_{soil}} = 0.071$ $p_{E_{mem}} = 0.051$ $p_l = 0.257$ $p_{.q_{sim}} = 0.034$ $p_{.\tau_{max}} = 0.068$	82.33	55.23
2	$f_{sim} = a_0 + a_1 \cdot \emptyset + a_2 \cdot d + a_3 \cdot \beta + a_4 \cdot E_{soil} + a_5 \cdot E_{mem} + a_6 \cdot l + a_7 \cdot q_{sim} + a_8 \cdot \tau_{max}$ $p_{a0} = 0.576$ $p_\emptyset = 0.088$ $p_d = 0.205$ $p_\beta = 0.115$ $p_{E_{soil}} = 0.070$ $p_{E_{mem}} = 0.049$ $p_l = 0.177$ $p_{.q_{sim}} = 0.038$ $p_{.\tau_{max}} = 0.079$	82.62	57.07
3	$f_{sim} = a_0 + a_1 \cdot \emptyset + a_2 \cdot \beta + a_3 \cdot E_{soil} + a_4 \cdot E_{mem} + a_5 \cdot l + a_6 \cdot q_{sim} + a_7 \cdot \tau_{max}$ $p_{a0} = 0.199$ $p_\emptyset = 0.187$ $p_\beta = 0.237$ $p_{E_{soil}} = 0.132$ $p_{E_{mem}} = 0.029$ $p_l = 0.268$ $p_{.q_{sim}} = 0.038$ $p_{.\tau_{max}} = 0.034$	80.88	57.39
4	$f_{sim} = a_0 + a_1 \cdot \emptyset + a_2 \cdot \beta + a_3 \cdot E_{soil} + a_4 \cdot E_{mem} + a_5 \cdot q_{sim} + a_6 \cdot \tau_{max}$ $p_{a0} = 0.025$ $p_\emptyset = 0.332$ $p_\beta = 0.389$ $p_{E_{soil}} = 0.167$ $p_{E_{mem}} = 0.014$ $p_{.q_{sim}} = 0.001$ $p_{.\tau_{max}} = 0.001$	80.13	47.04

5	$f_{sim} = a_0 + a_1 \cdot \emptyset + a_2 \cdot E_{soil} + a_3 \cdot E_{mem} + a_4 \cdot q_{sim} + a_5 \cdot \tau_{max}$ $p_{a0} = 0.014 \quad p_{\emptyset} = 0.542 \quad p_{E_{soil}} = 0.239 \quad p_{E_{mem}} = 0.007 \quad p_{\cdot q_{sim}} = 0.001 \quad p_{\cdot \tau_{max}} = 0.001$	80.64	64.29
6	$f_{sim} = a_0 + a_1 \cdot E_{soil} + a_2 \cdot E_{mem} + a_3 \cdot q_{sim} + a_4 \cdot \tau_{max}$ $p_{a0} = 0.001 \quad p_{E_{soil}} = 0.275 \quad p_{E_{mem}} = 0.004 \quad p_{\cdot q_{sim}} = 0.001 \quad p_{\cdot \tau_{max}} = 0.000$	81.45	70.93
7	$f_{sim} = a_0 + a_1 \cdot E_{mem} + a_2 \cdot q_{sim} + a_3 \cdot \tau_{max}$ $p_{a0} = 0.001 \quad p_{E_{mem}} = 0.003 \quad p_{\cdot q_{sim}} = 0.001 \quad p_{\cdot \tau_{max}} = 0.000$	81.01	72.06
8	$f_{sim} = a_0 + a_1 \cdot E_{mem} + a_2 \cdot \tau_{max}$ $p_{a0} = 0.011 \quad p_{E_{mem}} = 0.055 \quad p_{\tau_{max}} = 0.001$	55.27	24.10
9	$f_{sim} = a_0 + a_1 \cdot \tau_{max}/E_{mem}$ $p_{a0} = 0.000 \quad p_{\tau_{max/E_{mem}}} = 0.000$	76.33	72.52
10	$\mathbf{f_{sim} = a_1 \cdot \tau_{max}/E_{mem}}$ $\mathbf{a_1 = 0.005485 \quad p_{\tau_{max/E_{mem}}} = 0.000}$	**90.22**	**89.27**
11	$f_{sim} = a_1 \cdot \sqrt{q/E_{mem}}$ $p_{q_{/E_{mem}}} = 0.000$	80.68	76.98

The final expression, considering the coefficient obtained from the regression model is:

$$f_{sim} = 0.005485 \cdot \tau_{max}/E_{mem} \qquad \text{(Eq. 3)}$$

The units used for the regression model are kPa for both τ_{max}, and E_{mem}. The results for f_{sim} will be expressed in m according to the coefficient used. Table 6 shows the fulfilment of the 5 conditions for regression models that only depend on one variable, in this case $x = \tau_{max}/E_{mem}$. (Eq. 3) shows a logical and predictable relationship that shows that membrane deformation grows when tensile stress on membrane increases (which comes from high impact forces) and when the elastic modulus of membrane decreases.

Table 6.- Regression model $of\ f_{sim}\ vs.\ x,$ where $x = \tau_{max}/E_{mem}$. Conditions fulfilment.

Hypothesis	**Type of test**	**Criteria**	**Value**	**Fulfil?**
Normality of error distribution	Normality test (Anderson-Darling)	p > 0.05	p = 0.177	Yes
Null average of errors	Statistical hypothesis test H_0: μ_{errors} =0	p > 0.05	p = 0.423	Yes
Independence of errors in relation to response	Regression model between errors and response	p > 0.05	p = 0.221	Yes
Independence of errors in relation to predictive variables (homoscedasticity)	Regression model between errors and predictive variables	p > 0.05	p = 1.000	Yes
Independence of errors among them	Durbin-Watson ($d_{U\alpha}$=1.54)	$d > d_{U\alpha}$ $4-d > d_{U\alpha}$	d = 2.094	Yes

4.- Comparison between LE and SPH simulations

The aim of this section is to compare numerical simulations using SPH versus a traditional design method such as LE analysis. An infinite slope was considered for comparison, since various manufacturers adopt this method for design purposes. The variable adopted to compare both methods was the normal pressure applied to the ground that stabilises the unstable mass. Since cohesion and pore water pressures cannot been introduced in Autodyn, they were not considered either in the LE analysis or SPH numerical models. According to the tables provided by Da Costa & Sagaseta (2010), the error between considering an infinite slope and a limited height slope for the earth pressure, could be accounted for approximately 70% when the ratio H/d (slope height/depth of unstable fringe) is around 7.5. This H/d ratio of 7.5 represents the situation when $\beta = 30º$, $d = 2m$, which will provide the lowest value of H/d. The higher the value of H/d, the smaller the difference between infinite slope model and a limited height model. Infinite slope will provide higher values of earth pressure than those calculated with limited height slopes.

In the LE method, pressure q was calculated (Fig. 6) from the force balance equations considering Coulomb failure criterion in the slip surface:

$$\sum F_y = 0 \;\rightarrow\; \sigma \cdot a - q \cdot a - m \cdot g \cdot cos\beta = 0$$

$$m = d \cdot a \cdot \rho$$

$$\sum F_x = 0 \;\rightarrow\; \tau \cdot a - m \cdot g \cdot sin\beta = 0$$

$$\tau = \sigma \cdot tan\emptyset$$

$$(q \cdot a + m \cdot g \cdot cos\beta) \cdot tan\emptyset = m \cdot g \cdot sin\beta$$

$$q = d \cdot \rho \cdot g \cdot \left(\frac{sin\beta}{tan\emptyset} - cos\beta\right) \quad \text{(Eq. 4)}$$

Where q is the pressure normal to the slope surface that guarantees the equilibrium of the potential unstable fringe, d is the depth of the unstable fringe (see Fig. 6), ρ is the soil density, $\emptyset$ is the friction angle in the slip surface and β is the slope angle with respect to the horizontal. The pressure q is expressed per unit width of slope.

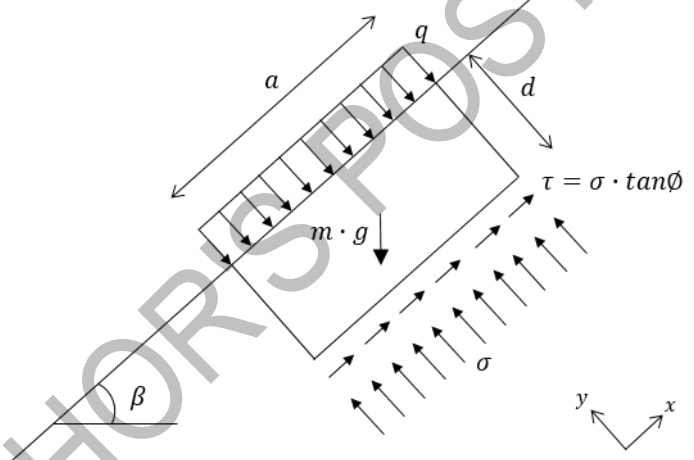

Fig. 6. LE method. Infinite slope. Force scheme.

In Table 7 the comparison between numerical simulation and infinite slope mode is shown. The term q_{sim} represents the normal pressure exerted by membrane to the ground considering the numerical simulation results and (Eq. 1) . The term q_{inf} represents the value of normal pressure that stabilises a potential earth fringe parallel to the slope surface, using the LE equation considering an infinite slope (Eq. 4).

Table 7.- Comparison between numerical simulations and infinite slope model

RUN	$\emptyset$ (º)	ρ (T/m^3)	d (m)	β (º)	E_{soil} (kPa)	E_{mem} (kPa)	l (m)	q_{sim} (kPa)	q_{inf} (kPa)
1	10	1.6	1	30	$5{\cdot}10^3$	200	2	40.48	30.92
2	30	1.6	1	30	$5{\cdot}10^6$	200	4	0.03	0.00
3	10	2.2	1	30	$5{\cdot}10^6$	600	2	27.84	42.51
4	30	2.2	1	30	$5{\cdot}10^3$	600	4	0.07	0.00
5	10	1.6	2	30	$5{\cdot}10^6$	600	4	45.12	61.83
6	30	1.6	2	30	$5{\cdot}10^3$	600	2	0.00	0.00
7	10	2.2	2	30	$5{\cdot}10^3$	200	4	68.63	85.02
8	30	2.2	2	30	$5{\cdot}10^6$	200	2	0.00	0.00
9	10	1.6	1	60	$5{\cdot}10^3$	600	4	115.04	69.24
10	30	1.6	1	60	$5{\cdot}10^6$	600	2	6.74	15.70
11	10	2.2	1	60	$5{\cdot}10^6$	200	4	42.64	95.21
12	30	2.2	1	60	$5{\cdot}10^3$	200	2	55.46	21.58
13	10	1.6	2	60	$5{\cdot}10^6$	200	2	79.28	138.49
14	30	1.6	2	60	$5{\cdot}10^3$	200	4	55.25	31.39
15	10	2.2	2	60	$5{\cdot}10^3$	600	2	262.09	190.42
16	30	2.2	2	60	$5{\cdot}10^6$	600	4	19.66	43.16
17	20	1.9	1.5	45	2502500	400	3	37.39	34.55

Fig. 7 compares SPH regression models derived from numerical simulations versus the LE model. In the vertical axis the normal pressure applied to the ground (q) divided by soil density (ρ) and unstable fringe depth (d) is represented. In the horizontal axis the slope angle with respect to horizontal (β) and also the friction angle ($\emptyset$) are represented. In relation to the regression models based on the numerical simulations, two surfaces have been depicted: g_{200} and g_{600}. Each one represents an elastic membrane with a Young Modulus of 200 kPa and 600 kPa respectively substituting these two values on (Eq. 2). LE model for an infinite slope is represented through g_{inf} surface (Eq. 4). In addition, individual points resulting from the simulation have been also depicted.

As we can see in Fig. 7, numerical simulations are dependent on membrane stiffness; the higher the Young Modulus of the membrane, the higher the normal force it is able to

exert to the ground. A possible explanation to this behaviour is that the higher the membrane stiffness, the higher the deceleration in the unstable mass during the impact against the membrane. This higher deceleration implies a higher impact force. The dynamic influence of the impact force can also be found in the evolution of the tensile stress on membrane vs. time, as depicted in Fig. 3. Obviously, in LE model, membrane stiffness and dynamic effects on impact forces cannot be considered. Differences between LE and SPH become greater when $\emptyset$ is low and β is high, showing a logical correlation between the physical phenomena and the numerical simulation results. Finally, the LE model provides higher values (for most of the β and $\emptyset$ range) than the SPH simulations when the membrane stiffness is below, approximately, 450 kPa. For stiffer membranes, LE simulations provides lower values.

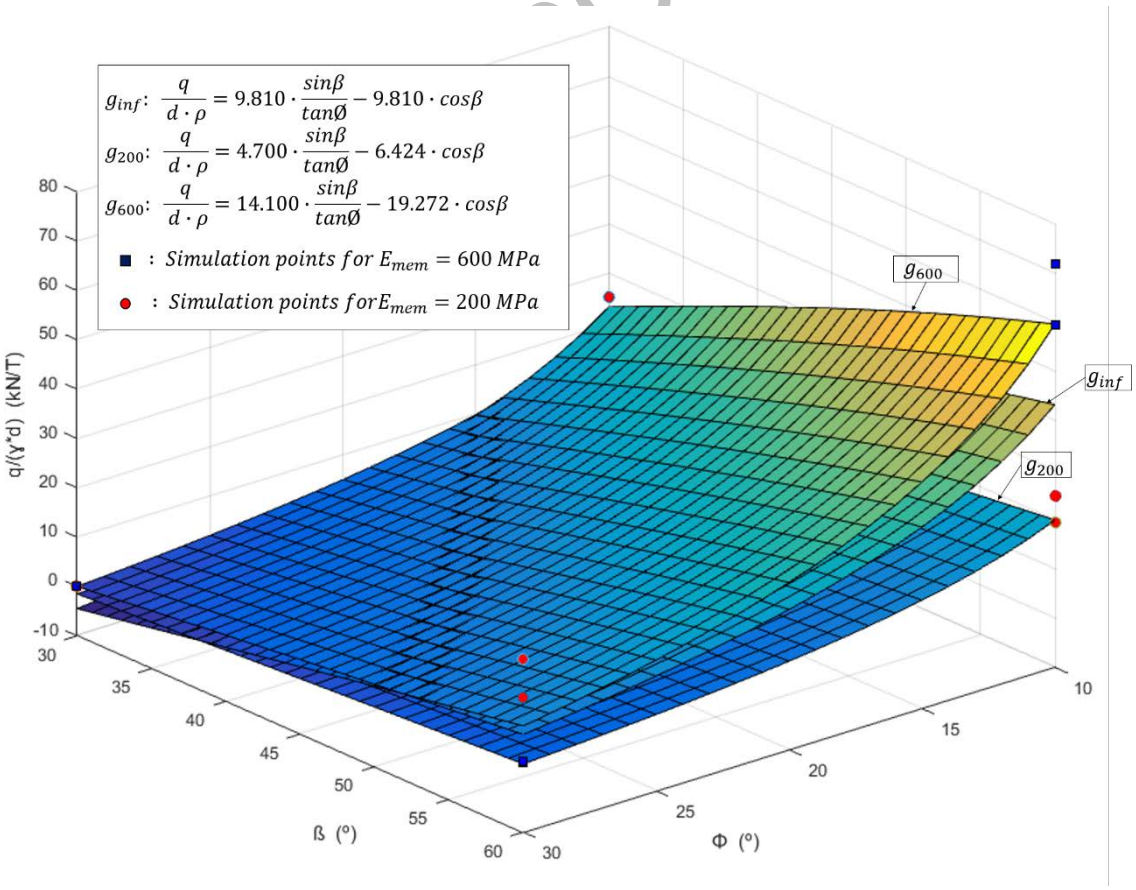

Fig. 7. Comparison of numerical simulation models (g_{200}, g_{600}) and LE model (g_{inf}). Single points from simulations also depicted.

5.- Conclusions

A simulation method for obtaining the maximum tensile stress on a membrane anchored to the ground for soil slope stabilisation has been suggested. To the best knowledge of the authors, this method has been used for the first time for the simulation of flexible membranes anchored to soil slopes. The unstable mass has been discretised though SPH. 17 different numerical simulations have been carried out based on a DOE. An unstable fringe of ground parallel to the slope surface has been assumed. Slope length was limited to 30 m.

A regression model that modelises the pressure normal to the ground q_{sim} formed by 17 runs results has been generated. This model depends linearly on two variables, which have been generated through a combination of the following physical values: unstable mass depth, ground density, friction angle, slope angle and elastic modulus of membrane. Elastic modulus of ground and bolt separation did not show a significant influence in the regression model. The apparent lack of influence of bolt separation could be due to an insufficient number of runs in the DOE. On the other hand, it is considered that the internal failures inside the unstable mass have more influence in q_{sim} rather than the elastic modulus of the soil itself.

Besides, a regression model that correlates maximum deformation on membrane, (deformation normal to the ground on the mid point of a membrane panel) in relation to its maximum tensile stress and elastic modulus has also been included, demonstrating a physical logical relationship.

In addition, comparison between numerical simulation results and LE analysis considering an infinite slope has been also discussed. The results obtained with the LE differs from those obtained with SPH simulations and differences get larger for low $\emptyset$ and high β. For high stiff membranes, LE method would underestimate the maximum pressure, while for low stiff membranes the LE method would overestimate this maximum pressure.

To conclude, one of the main drawbacks of using the LE method, in spite of its simplicity, is that it does not consider the membrane stiffness, while numerical simulations performed in this paper showed that this variable has a significant influence on the normal pressure applied to the slope surface.

Acknowledgements

The realization of this research paper has been possible thanks to the funding of the following entities: SODERCAN (Sociedad para el Desarrollo de Cantabria), Consejería de Obras Públicas del Gobierno de Cantabria, Iberotalud S.L., Malla Talud Cantabria S.L. and Contratas Iglesias S.L.

The authors wish also to acknowledge the support provided by the GICONSIME Research Group of the University of Oviedo and the GITECO Research Group of the University of Cantabria. We also thank Swanson Analysis Inc. for the use of the ANSYS Academic program.

References

Bertolo P., Giacchetti G., 2008. An approach to the design of nets and nails for surficial rock slope revetment. Interdisciplinary Workshop on Rockfall Protection, June 23-25, 2008, Morshach, Switzerland.

Bertolo, P., Oggeri, C., Peila, D., 2009. Full-scale testing of draped nets for rock fall protection Canadian Geotechnical Journal, 46 (3), pp. 306-317.

Bui, H.H., Fukagawa, R., Sako, K., Ohno, S., 2008a. Lagrangian meshfree particles method (SPH) for large deformation and failure flows of geomaterial using elastic-plastic soil constitutive model. International Journal for Numerical and Analytical Methods in Geomechanics, 32 12), pp. 1537-1570.

Bui, H.H., Sako, K., Fukagawa, R., Wells, J.C., 2008b. SPH-based numerical simulations for large deformation of geomaterial considering soil-structure interaction. 12th International Conference on Computer Methods and Advances in Geomechanics 2008, 1, pp. 570-578.

Bui, H.H., Fukagawa, R., Sako, K., Wells, J.C. 2011. Slope stability analysis and discontinuous slope failure simulation by elasto-plastic smoothed particle hydrodynamics (SPH) Geotechnique, 61 (7), pp. 565-574.

Blanco-Fernandez, E., Castro-Fresno, D., Díaz, J.J.D.C., Lopez-Quijada, L., 2011. Flexible systems anchored to the ground for slope stabilisation: Critical review of existing design methods Engineering Geology, 122 (3-4), pp. 129-145.

Blanco-Fernandez, E., Castro-Fresno, D., Del Coz Díaz, J.J., Díaz, J., 2013. Field measurements of anchored flexible systems for slope stabilisation: Evidence of passive behaviour. Engineering Geology, 153, pp. 95-104.

Bojanowski, C., 2014. Numerical modeling of large deformations in soil structure interaction problems using FE, EFG, SPH, and MM-ALE formulations. Archive of Applied Mechanics, 84 (5), pp. 743-755.

Castro Fresno, D., 2000. Estudio y análisis de las membranas flexibles como elemento de soporte para la estabilización de taludes y laderas de suelos y/o materiales sueltos. PhD thesis, Universidad de Cantabria, Santander.

Da Costa García, A., 2004. Inestabilidades por degradación superficial de taludes en suelos. Corrección mediante sistemas de refuerzo anclados. PhD thesis, Universidad de Cantabria, Santander.

Da Costa, A., Sagaseta, C., 2010. Analysis of shallow instabilities in soil slopes reinforced with nailed steel wire meshes. Engineering Geology, 113 (1-4), pp. 53-61.

Dakssa, L.M., Harahap, I.S.H., 2012. Investigating rainfall-induced unsaturated soil slope instability: A meshfree numerical approach. WIT Transactions on Engineering Sciences, 73, pp. 231-242.

Gray J.P., Monaghan J.J., Swift R.P., 2001. SPH elastic dynamics. Computer Methods in Applied Mechanics and Engineering, 190 (49-50), pp. 6641-6662.

Jewell, R. A., and Pedley, M. J., 1990. Soil nailing design-the role of bending stiffness. Ground Engineering, 22(10), 30-36.

Juran, I., Baudrand, G., Farrag, K., and Elias, V., 1990. Kinematical limit analysis for design of soil-nailed structures. J.Geotech.Eng., 116(1), 54-72.

Liang, D.-F., He, X.-Z., 2014. A comparison of conventional and shear-rate dependent Mohr-Coulomb models for simulating landslides. Journal of Mountain Science, 11 (6), pp. 1478-1490.

Luis Fonseca, R. J., 2010. Aplicación de Membranas Flexibles para la Prevención de Riesgos Naturales. Geobrugg Ibérica, S.A., Madrid.

Monaghan, J.J., 2000. SPH without a tensile instability. Journal of Computational Physics, 159 (2), pp. 290-311.

Muhunthan, B., Shu, S., Sasiharan, N., Hattamleh, O. A., Badger, T. C., Lowell, S. M., and Duffy, J. D., 2005. Analysis and design of wire mesh/cable net slope protection. Rep. No. WA-RD 612.1, Washington State Transportation Center (TRAC), Seattle, Washington, USA.

Nonoyama, H., Moriguchi, S., Sawada, K., Yashima, A., 2015. Slope stability analysis using smoothed particle hydrodynamics (SPH) method. Soils and Foundations, 55 (2), pp. 458-470.

Phear, A., Dew, C., Ozsoy, B., Wharmby, N. J., Judge, J., and Barley, A. D., 2005. Soil nailing - best practice guidance. Rep. No. C637, CIRIA, London.

Sasiharan, N., Muhunthan, B., Badger, T. C., Shu, S., and Carradine, D. M., 2006. Numerical analysis of the performance of wire mesh and cable net rockfall protection systems. Eng.Geol., 88(1-2), 121-132.

Schlosser, F., 1983. Analogies et differences dans le comportement et le calcul des ouvrages de soutennement en terre armee et par clouage du sol. Annales de l'Institut Technique du Bâtiment et des Travaux Publiques, (148), 26-38.

UNI 11437:2012. Rockall protection measures: Tests on meshes for slope coverage. UNI (Ente Nazionale Italiano di Unificazione), 2012.

Wang, B. and Men, Y., 2010. Analysis on internal stability of anchors in clay. Xi'an Jianzhu Keji Daxue Xuebao/Journal of Xi'an University of Architecture and Technology, 42(3), 382-386.

Wei, L., Chen, C., Xu, J., and Hu, S., 2008. Study on strength reduction FEM considering seepage and bolt. Yanshilixue Yu Gongcheng Xuebao/Chinese Journal of Rock Mechanics and Engineering, 27(SUPPL. 2), 3471-3476.

Wu, Q., An, Y., Liu, Q.-Q., 2015. SPH-based simulations for slope failure considering soil-rock interaction. Procedia Engineering, 102, pp. 1842-1849.

Zhang, W.J., Maeda, K., 2014. The model test and SPH simulations for slope and levee failure under heavy rainfall considering the coupling of soil, water and air. Geotechnical Special Publication, (236 GSP), pp. 538-547.